Annals of Clinical and Analytical Medicine
Original Research

Effect of implant-abutment connections with peri-implant bone defect models under removal torque force: A 3D finite element analysis

Ahu Uraz Çörekci[1], Sila Cagri Isler[2], Janset Şengül[3], Berceste Guler[4], Yücel Özdemir[5], Deniz Ozbay[2]
[1] Department of Periodontology, Faculty of Dentistry, Izmir Democracy University, Izmir
[2] Department of Periodontology, Faculty of Dentistry, Gazi University, Ankara
[3] Department of Periodontology, Ankara Memorial Hospital, Ankara
[4] Department of Periodontology, Faculty of Dentistry, Kütahya Health Sciences University, Kütahya
[5] Department of Private Practice, Istanbul, Turkey

Abstract

Aim: Peri-implant complications can result in a process that includes implant removal and is related to anatomical conditions, implant design, remaining peri-implant bone and defect type, and bone quality. The aim of this study was to assess how different implant geometries and thread designs in different peri-implant bone defect types under a removal torque value could affect the stress distributions in the implants and surrounding bone employing finite element analysis (FEA).

Material and Methods: Four different designs (Type-I: external hexagonal-cylindrical; Type-II: internal hexagonal-root form; Type-III: internal conical-cylindrical; Type-IV: Internal conical-root form) placed in the maxillary and mandibular posterior region with D2 and D3 type bone with three peri-implant bone defect models or as a control, fully osseointegrated dental implants were evaluated using the 3D-FEA method. The application of a reverse torque force of 10 Ncm to implants has been examined by comparing the stress distributions of the maximum principle and the minimum principle.

Results: The stress transmitted to the cortical bone in the neck region was found to be higher than to the cancellous bone. Circular-type bone defects had an increasing trend for stress values towards the apical region. Type II and Type IV implants demonstrated the highest von Mises stress values in peri-implant defect models, especially on buccal sites.

Discussion: In the presence of horizontal and circular bone defects, the implant surface reached higher stress values in 2/3 coronal sites remarkably for the root-form implants during implant removal. Reaching high-stress values in the buccal area has marked the critical importance of buccal bone preservation during implant removal procedures.

Keywords

Dental Implants, Removal Torque, Peri-Implantitis, Finite Element Analysis, Abutment Connection

DOI: 10.4328/ACAM.21527 Received: 2022-11-30 Accepted: 2023-01-05 Published Online: 2023-01-24 Printed: 2023-04-01 Ann Clin Anal Med 2023;14(4):358-364
Corresponding Author: Ahu Uraz Çörekçi, Department of Periodontology, Faculty of Dentistry, Izmir Demokrasi University, Konak, Izmir, Turkey.
E-mail: ahu.urazcorekci@idu.edu.tr P: +90 232 260 10 01
Corresponding Author ORCID ID: https://orcid.org/0000-0001-6281-6855

Introduction

Peri-implantitis is defined as an inflammatuar disease of functionally loaded dental implants and characterized by inflammation of the mucosa and subsequent progressive supporting bone loss that may eventually lead to a complete loss of osseointegration [1].

Implant removal may also be demonstrated if the implants are immobile, but the fixture is broken, misplaced, infected or has advanced peri-implantitis. In these cases, the implant may remain osseointegrated, and removal of the implants may cause damage to the surrounding tissues, leading to eventual loss of valuable soft and hard tissue volume [2]. Although various techniques and their combinations have been reported to explant a failed dental implant, the selection of the appropriate removal technique should be addressed based on factors including anatomical conditions, implant design, bone quality, and the amount of bone remaining around the implant [1,3]. Determination of the most appropriate minimally invasive technique is critical for preserving the available bone and gingival tissues at the site, where the implant has been removed [4].

Considering the application of optimal reverse torque force without any damage to the surrounding bone during the removal of an implant, the effect of implant geometry and thread designs in different types of peri-implant bone loss is of great clinical relevance. The distribution and stress magnitude on the implant and peri-implant bone surrounding in different clinical situations can be evaluated by means of finite element analysis (FEA), which provides comprehensive predictions of complex implant-bone system relations depending on the accuracy in modeling the implant and bone structure design [5,6].

The aim of the present study was to assess how different implant geometries and thread designs in different peri-implant bone defect types under removal torque could affect the stress distributions in the implants and surrounding bone employing FEA.

Material and Methods

Four different implant designs placed in the maxillary and mandibular posterior region with D2 and D3 type bone [7] with different types of defects or without a bone defect were evaluated using the 3D FEA method. For this purpose, a total of 32 models were obtained by creating three different peri-implant bone defect shapes around each implant and a control group without defects. Von Mises stress, maximum principle and minimum principal stress distributions formed in the cortical and cancellous bone around the implant on the implant surface by applying a 10 Ncm reverse torque force on the implants in these models were examined by FEA, and the stress distributions were compared.

The implant and implant-abutment connection designs were defined as follows:

• Implant Type I: Cylindrical body, square-thread, bone-level, external connection (external hexagon), length 10.5 mm, 4mm ø (External [Maestro] Dental Implants, BioHorizons, Birmingham, AL, USA.),

• Implant Type II: Root-form, tapered body, buttress thread, bone-level, internal connection (internal hexagon), length 10.5 mm, 3.8 mm ø (Laser-Lok Tapered Internal, BioHorizons Implant System),

• Implant type III: Cylindrical body, micro-macro V-shaped thread, bone-level, internal conical connection, length 11 mm, 4 mm ø, (Microcone, Medentika, Medentika GmbH, Hügelsheim, Germany),

• Implant type IV: Root-form, tapered body, V-shaped micro-threaded in coronal portion and macro-threaded in apical portion, bone-level, internal conical connection, length 11 mm, 4.3 mm ø, (Quattrocone, Medentika Implant System).

Four peri-implant bone defect models were determined based on the classification by Schwarz et al. (2010) [8].

• Type A: Loss of 50% of the buccal bone–vertical dehiscence (Class Ic)

• Type B: Loss of 50% -horizontal dehiscence (Class II)

• Type C: Loss of 50% peri-implant region, a circumferential component of the defect (Class Ie)

• Type D: No bone loss, completely osseointegrated.

Maxilla, mandible, and implants and their components were scanned using a smart optics scanner (Activity 880, Smart Optics, Sensortechnik GmbH, Bochum, Germany). Cone beam computerized tomography images were transferred to a 3-D reconstruction software (3D-Doctor; Able Software Corp, Lexington, MA) and were converted into Hounsfield units with the 'Interactive Segmentation' method to determine the bone tissue. The models were placed in the correct coordinates in 3D space in Rhinoceros 4.0 and VRMesh (VirtualGrid Inc, Bellevue City WA, USA) software and the modeling process was completed. Then, they were transferred to Algor Fempro (ALGOR, Inc. 150 Beta Drive Pittsburgh, PA 15238-2932 USA) software in stl format to make them ready for analysis.

The models were meshed with modeling software. In the meshing process, the models are formed from elements with 10 nodes (brick type) as much as possible. In the regions close to the center of structures in models, elements with fewer nodes are used to complete the structure when necessary. The vertical and narrow regions in the models, which facilitate the analysis process, were made regular by removing linear elements.

A 10 Ncm counter-clockwise force was applied to remove the implants. The material properties used in the models were homogeneous, isotropic and linear elastic. The strength capacity of the cortical bone was accepted as 121-135 MPa for maximum principle (tensile) stresses, between 167-205 MPa for minimum principle (compression) forces, and as maximum 20 MPa for cancellous bone. The amount of force required for the resistance capacities of the stress values to be obtained in the analysis of the models accepted as linear elastic was calculated with a proportional increase.

The maximum principle, minimum principle and von Mises stresses and their distributions were calculated resulting from the application of CTRT. The values obtained from these circumferential measurements were compared by determining 4 reference points (mesial, buccal, distal, lingual/palatal) around each implant and were marked as the maximum and minimum stresses.

The stress distribution was depicted into colorimetric scales in order to allow the comparison of the differences among study models.

Results

When evaluating the stress values of the Type I implant in the mandible according to the peri-implant defect types, the highest von Mises stress value was exhibited in the circular defect model in 2/3 coronal part of the implant (5.88 MPa). The highest stress value observed in the neck region for this implant type was in the buccal model as in the maxilla. Type II implant showed a markedly higher stress value in the 2/3 coronal part of the implant in the circular defect model compared to the other models (20.02 MPa). Another high-stress value was seen

Table 1. Comparison of maximum stress values in the neck and apical regions of the implant, cancellous and cortical bone in peri-implant defect and control models in the maxilla.

			Neck region				Apical			
			Buccal	Mesial	Palatal	Distal	Buccal	Mesial	Palatal	Distal
Type I	Buccal defect	Implant	1.289	2.108	2.536	2.335	0.415	0.646	0.781	0.552
		Cortical bone		3.351	4.755	3.504		0.385	0.621	0.415
		Cancellous bone		0.366	0.458	0.413	0.103	0.170	0.302	0.151
	Horizontal defect	Implant	2.852	4.265	5.627	4.260	1.173	1.479	1.419	0.977
		Cortical bone	6.035	6.708	8.286	5.308	0.838	0.930	0.875	0.658
		Cancellous bone	0.650	0.641	0.813	0.700	0.255	0.632	0.363	0.319
	Circular defect	Implant	0.402	0.516	0.130	0.401	3.369	2.934	3.413	2.109
		Cortical bone	0.102	0.061	0.103	0.056	0.058	0.018	0.034	0.018
		Cancellous bone	1.418	1.722	1.501	1.323	0.411	0.644	0.886	0.504
	Control	Implant	7.012	3.953	1.396	5.130	0.496	0.524	0.378	0.260
		Cortical bone	3.599	2.063	2.231	2.188	0.543	0.278	0.308	0.293
		Cancellous bone	0.238	0.160	0.148	0.138	0.196	0.118	0.077	0.134
Type II	Buccal defect	Implant	1.206	3.188	4.003	4.032	1.014	1.022	2.608	0.991
		Cortical bone		3.111	3.646	3.022		0.355	0.621	0.369
		Cancellous bone		0.539	0.624	0.530	0.075	0.133	0.185	0.135
	Horizontal defect	Implant	7.798	11.067	7.404	7.164	10.327	11.802	20.032	7.946
		Cortical bone	6.954	10.837	8.311	7.531	0.916	0.886	1.031	0.933
		Cancellous bone	0.698	0.848	0.808	0.785	0.153	0.431	0.438	0.343
	Circular defect	Implant	0.439	0.260	0.129	0.251	4.625	4.700	4.768	3.956
		Cortical bone	0.065	0.055	0.046	0.058	0.059	0.019	0.030	0.018
		Cancellous bone	1.301	1.245	1.541	1.185	0.440	0.776	0.601	0.577
	Control	Implant	7.020	5.278	3.080	3.826	0.965	0.728	0.634	0.754
		Cortical bone	3.155	2.151	2.997	2.193	0.495	0.263	0.277	0.276
		Cancellous bone	0.600	0.391	0.445	0.538	0.111	0.071	0.043	0.084
Type III	Buccal defect	Implant	0.557	1.782	2.283	1.936	0.689	0.937	2.264	1.106
		Cortical bone		2.016	2.826	1.670		0.236	0.478	0.204
		Cancellous bone		0.700	0.763	0.628	0.058	0.149	0.191	0.187
	Horizontal defect	Implant	3.972	2.040	2.820	4.244	0.967	1.304	2.563	1.920
		Cortical bone	5.026	3.871	4.010	4.505	0.766	0.683	1.263	0.598
		Cancellous bone	0.488	0.535	0.589	0.609	0.159	0.298	0.356	0.187
	Circular defect	Implant	0.110	0.106	0.143	0.194	1.501	2.063	3.243	2.016
		Cortical bone	0.068	0.058	0.035	0.049	0.017	0.019	0.044	0.017
		Cancellous bone	0.960	0.785	0.859	0.992	0.214	0.422	0.642	0.440
	Control	Implant	3.228	4.894	2.892	3.383	0.552	0.920	1.370	0.902
		Cortical bone	1.253	2.015	1.308	1.125	0.203	0.177	0.352	0.286
		Cancellous bone	0.545	0.824	0.492	0.530	0.0735	0.131	0.213	0.155
Type IV	Buccal defect	Implant	0.772	1.908	2.216	2.840	0.464	0.767	1.194	1.069
		Cortical bone			2.958	2.046		0.269	0.486	0.253
		Cancellous bone		0.744	0.760	0.604	0.033	0.1301	0.211	0.101
	Horizontal defect	Implant	7.282	5.425	3.914	6.242	0.411	1.229	2.320	2.063
		Cortical bone	8.352	7.664	6.165	5.569	0.825	0.496	1.699	0.694
		Cancellous bone	0.685	0.501	0.510	0.529	0.129	0.149	0.208	0.199
	Circular defect	Implant	0.089	0.128	0.112	0.101	1.071	1.632	2.957	3.447
		Cortical bone	0.111	0.072	0.024	0.060	0.115	0.022	0.019	0.021
		Cancellous bone	1.305	1.047	0.906	0.939	0.133	0.268	0.309	0.324
	Control	Implant	9.339	4.878	3.928	6.264	0.503	0.438	0.956	1.129
		Cortical bone	2.585	1.591	1.500	1.482	0.040	0.211	0.245	0.183
		Cancellous bone	0.640	0.529	0.581	0.576	0.023	0.103	0.086	0.095

Table 2. Comparison of maximum stress values in the neck and apical regions of the implant, cancellous and cortical bone in peri-implant defect and control models in the mandible.

			Neck region				Apical			
			Buccal	Mesial	Palatal	Distal	Buccal	Mesial	Palatal	Distal
Type I	Buccal defect	Implant	1.758	4.931	2.210	3.744	0.166	0.243	0.312	0.156
		Cortical bone		2.304	1.731	1.899		1.053	1.344	1.009
		Cancellous bone		0.998	0.718	0.831	0.035	0.055	0.084	0.020
	Horizontal defect	Implant	5.465	4.527	4.022	4.902	1.029	1.128	1.167	0.716
		Cortical bone	4.919	7.067	4.706	3.188	1.668	1.194	1.666	1.538
		Cancellous bone	1.023	0.383	0.246	0.888	0.304	0.349	0.366	0.353
	Circular defect	Implant	0.142	0.087	0.056	0.206	1.188	1.091	1.257	0.829
		Cortical bone	0.076	0.028	0.034	0.025	0.230	0.023	0.249	0.022
		Cancellous bone	0.875	0.641	0.714	0.816	0.322	0.284	0.387	0.256
	Control	Implant	1.839	3.092	3.908	3.023	0.169	0.179	0.182	0.164
		Cortical bone	1.588	1.254	1.719	1.179	1.065	0.860	1.319	0.743
		Cancellous bone	0.422	0.407	0.624	0.506	0.048	0.050	0.070	0.047
Type II	Buccal defect	Implant	1.439	4.902	2.530	3.899	0.370	0.452	0.486	0.287
		Cortical bone		2.085	1.832	1.802		1.085	1.427	0.935
		Cancellous bone		0.813	0.746	0.729	0.109	0.112	0.125	0.084
	Horizontal defect	Implant	26.446	17.743	7.244	27.181	2.721	2.004	1.176	2.185
		Cortical bone	6.376	5.833	4.826	7.130	2.643	1.247	2.125	1.693
		Cancellous bone	0.660	0.433	0.617	1.177	0.273	0.194	0.233	0.219
	Circular defect	Implant	0.054	0.103	0.229	0.129	3.141	2.323	1.410	2.222
		Cortical bone	0.063	0.023	0.037	0.030	0.177	0.128	0.137	0.022
		Cancellous bone	0.754	0.878	1.078	0.721	0.443	0.450	0.465	0.423
	Control	Implant	1.410	2.394	2.912	2.705	0.370	0.342	0.157	0.357
		Cortical bone	1.438	1.456	1.606	1.371	1.520	0.844	1.116	0.664
		Cancellous bone	0.480	0.610	0.920	0.534	0.911	0.081	0.074	0.079
Type III	Buccal defect	Implant	0.180	2.075	1.583	2.101	0.366	0.521	1.012	0.497
		Cortical bone		1.045	0.908	1.427		0.514	0.869	0.398
		Cancellous bone		1.120	1.307	1.792	0.116	0.145	0.246	0.148
	Horizontal defect	Implant	3.916	3.553	4.243	4.097	0.875	1.227	2.106	1.507
		Cortical bone	1.470	2.537	4.172	2.671	1.489	1.169	1.540	1.044
		Cancellous bone	0.455	0.439	0.686	0.604	0.153	0.159	0.193	0.166
	Circular defect	Implant	0.118	0.094	0.080	0.089	0.828	1.278	1.627	1.462
		Cortical bone	0.072	0.023	0.038	0.027	0.098	0.020	0.157	0.020
		Cancellous bone	0.973	0.602	0.556	0.560	0.400	0.434	0.449	0.359
	Control	Implant	1.623	1.439	1.019	1.159	0.293	0.412	0.705	0.403
		Cortical bone	0.832	0.687	0.810	0.662	0.801	0.387	0.879	0.332
		Cancellous bone	0.942	0.919	0.838	0.829	0.084	0.098	0.109	0.057
Type IV	Buccal defect	Implant	0.1944	4.482	1.806	2.326	0.323	0.185	0.595	0.289
		Cortical bone		1.178	0.938	0.914		0.419	0.801	0.492
		Cancellous bone		0.914	0.831	0.706	0.033	0.028	0.039	0.027
	Horizontal defect	Implant	16.493	14.728	4.888	15.67	1.194	1.608	0.747	1.193
		Cortical bone	5.765	2.191	4.512	4.374	1.402	1.851	1.333	1.261
		Cancellous bone	0.422	0.411	0.385	0.189	0.178	0.305	0.154	0.248
	Circular defect	Implant	0.086	0.045	0.051	0.051	1.130	0.702	0.815	1.252
		Cortical bone	0.134	0.028	0.048	0.027	0.280	0.025	0.134	0.025
		Cancellous bone	1.210	0.901	1.063	1.012	0.121	0.120	0.111	0.091
	Control	Implant	0.919	2.347	1.140	1.803	0.254	0.139	0.196	0.240
		Cortical bone	0.703	0.864	0.722	0.701	0.778	0.316	0.636	0.365
		Cancellous bone	0.726	0.930	0.803	0.918	0.120	0.049	0.048	0.042

in the 2/3 region of the implant in horizontal defect (26.44 MPa). The highest stress values in Type III and Type IV implants were observed in circular defects in 2/3 coronal region of the implants and horizontal defects in 1/3 coronal region of the implants, respectively.

Regarding the maxilla, for all the types of implants, in the presence of a buccal defect, both in the neck and apical regions of the implant, cancellous and cortical bone, the highest stress values were observed in the palatal aspects. In the horizontal defects, the highest values were also identified in the palatinal

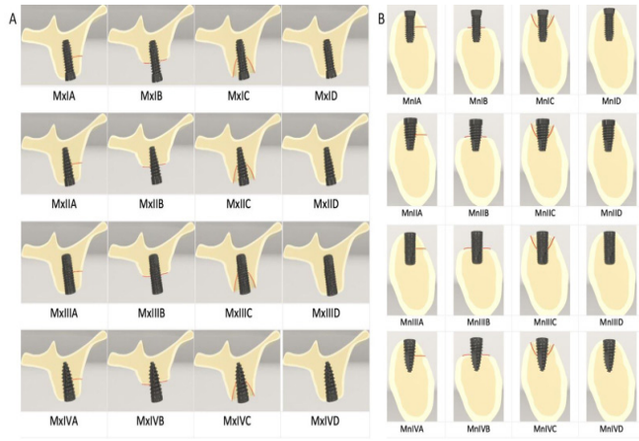

Figure 1. A. Models in the posterior region of the maxilla, MxIA: Type I implant-Type A defect; MxIB: Type I implant-Type B defect; MxIC: Type I implant-Type C defect; MxID: Type I implant-Type D defect; MxIIA: Type II implant- Type A defect; MxIIB: Type II implant- Type B defect; MxIIC: Type II implant-Type C defect; MxIID: Type II implant- Type D defect; MxIIIA: Type III- Type A defect; MxIIIB: Type III- Type B defect MxIIIC: Type III- Type C defect; MxIIID: Type III- Type D defect; MxIVA: Type IV implant-Type A defect; MxIVB: Type IV implant-Type B defect; MxIVC: Type IV implant-Type C defect; MxIVD: Type IV implant-Type D defect.

B. Models in the posterior region of the mandible, MnIA: Type I implant-Type A defect; MnIB: Type I implant-Type B defect; MnIC: Type I implant-Type C defect; MnID: Type I implant-Type D defect; MnIIA: Type II implant- Type A defect; MnIIB: Type II implant- Type B defect; MnIIC: Type II implant- Type C defect; MnIID: Type II implant- Type D defect; MnIIIA: Type III- Type A defect; MnIIIB: Type III- Type B defect MnIIIC: Type III- Type C defect; MnIIID: Type III- Type D defect; MnIVA: Type IV implant-Type A defect; MnIVB: Type IV implant-Type B defect; MnIVC: Type IV implant-Type C defect; MnIVD: Type IV implant-Type D defect.

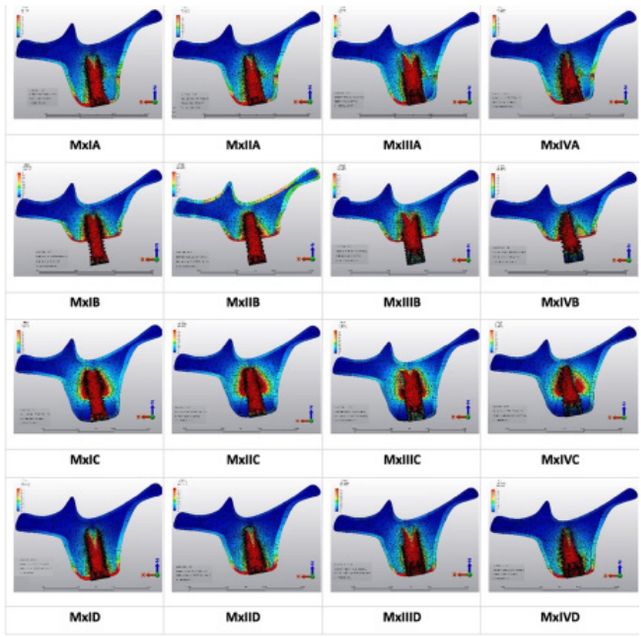

Figure 2. Calorimetric representation of the effects of stress distributions on cortical and cancellous bone in maxillary models.

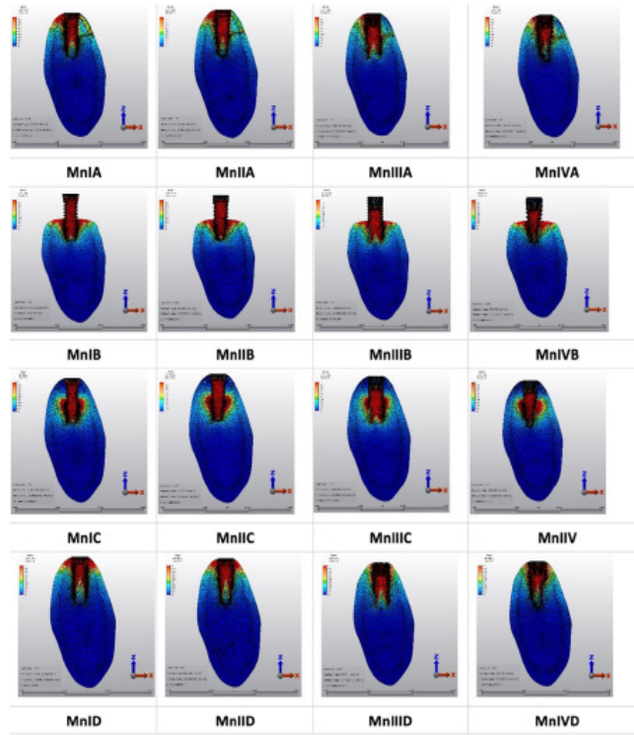

Figure 3. Calorimetric representation of the effects of stress distributions on cortical and cancellous bone in mandibular models.

aspects of the neck regions for the implant surface, and cancellous and cortical bone, while in the apical region of all sites of interest, mesial aspects showed the highest stress values for Type I implant. For Type IV implant, in the horizontal and circular defects, buccal aspects showed the highest stress for all sites in the neck region and palatal aspects had the highest values in the apical region. In the control models, in the neck regions of the implant surface, cancellous and cortical bone, the highest stress values were seen in the buccal aspects. (Figure 2 and Figure 3) In both horizontal and circular type defects, the maximum stress values were observed in palatal surface of Type II implant in the apical region (20.03 MPa, and 4.76 MPa). Among all the control models, the highest stress was seen in the buccal aspect of Type IV implants in the apical region (9.33 MPa). (Table 1)

When evaluating the mandibular models, in the presence of buccal defect, the highest stress values were exhibited in the mesial aspects of implant surface, cancellous and cortical bone in the neck region, while lingual sites presented the highest values for all sites in the apical region for Type I and II implants. For the Type I implants, in horizontal defects, the highest stresses were found in the buccal and distal aspects for the neck and apical regions, respectively. Whereas the highest stresses were observed in Type II implants in the opposite areas compared to Type I implants. For the Type III implants, in both buccal and horizontal defects, lingual aspects had the highest stresses for all sites of interest. For the Type IV implants, the highest stresses were found in the mesial and lingual aspects for the neck and apical regions, respectively. The lowest stress values of the mandible were observed in the cancellous bone in the presence of horizontal defect, while it was seen in the cortical bone in the presence of circular defect (Table 2).

Discussion

High torque applications are known to cause excessive compression of bone, inhibition of microcirculation, microdamage, the spread of programmed cell death over a wider area, prolongation of the inflammatory phase, delayed healing, and peri-implant marginal bone loss [9,10]. The present study demonstrated that the bone with D3 density modeled as the upper jaw has more intense and higher stress values compared to the bone with D2 density modeled as the lower jaw. Considering the values on the implant surface and surrounding cortical and cancellous bone together, the stress transmitted to the cortical bone in the neck region was found to be higher than cancellous bone. However, in the models where the implants are in contact with both the cortical and cancellous bone, the stresses were seen to distribute more regularly, while the stress values increased much more in the models where the implants are only in contact with the cancellous bone, especially in the maxilla models with circular-type defects. Besides, in the apical region, the stresses on the surface of the Type II and Type IV implants are greater than the other areas, especially in the palatal aspects. A study has reported the stress distributions in cortical and cancellous bone caused by bone resorption progressing from the marginal area of the implants towards the apical using finite element stress analysis [11]. In parallel with the present study findings, a study has demonstrated higher stress in the cortical bone than in the trabecular bone for narrow diameter implants placed in maxillary and mandibular models and the stress concentrations were showed at the top threads in the coronal third of the implants and the cortical bone-implant interface [12]. On the other hand, Lemos et al. (2021) stated that a progressive increase in peri-implant marginal bone loss was associated with higher stress concentrations in the bone tissue in the coronal and apical regions of the implants [13]. A study has examined the effect of the stress caused by occlusal forces in the presence of horizontal bone loss at different levels on peri-implant bone using three-dimensional FEA and found that as the amount of cortical bone decreased, the stress on implant surface increased [14]. Furthermore, in cases where the horizontal bone loss is seen exceeds 25% of the implant length, it has been shown that the stress on the implant surface reaches a level that could not compensate for functional forces [14]. In our study, it was observed that in horizontal and circular bone defect models, where 50% of the implant length is lost, the stress on the implant surface reached higher values, especially in root form tapered implants.

The present study exhibited that Type II implants mostly demonstrated the highest von Mises stress values compared to the other types of implants in the presence of maxillary peri-implant defects. However, the maximum value of stress was identified for Type IV in 2/3 coronal site, which was the area containing to the first BIC, in the presence of circular peri-implant defects among all the maxillary models. Moreover, in the control model without bone loss, the greatest stress was seen for the Type IV implant at the buccal aspect in the neck area. These findings marked that root-form tapered implant body with buttress thread or V-shaped thread indicated higher stress concentrations on the implant surface and surrounding bone compared to implants having cylindrical implant body in maxilla. One explanation for this finding may be that those conical tapered implants are more stabile increasing bone-implant contact during insertion through applying pressure on the cortical bone [15,16]. A study has indicated that the conical implants exhibited higher von Mises and maximum principal stresses in the peri-implant bone tissue in non-linear groups, while in linear groups the cylindrical implants showed greater stress compared to conical implants [15]. In the present study, in the presence of a horizontal defect, it should be considered that the high stress value in the remaining bone after removal of a conical tapered implant may not have a favourable healing potential to allow immediate implant placement [17]. Furthermore, reaching high stress values in the buccal area has marked the critical importance of buccal bone preservation during implant removal procedures.

The study has reported that the continuous increase in the dimension of the thread geometry and in the BIC area was associated with higher stress magnitude in the surrounding bone [18]. In that study, the highest stress value was demonstrated for the root-form tapered implant having a double-lead V-shape thread compared with other models presenting a tapered implant with micro-thread in the collar area, reverse buttress thread in the middle area. In both the maxilla and mandible, higher stress value in cortical bone was observed for the root-form, tapered body implant with buttress thread compared to the other implant types. Implant-abutment connection design is another critical factor influencing stress distributions on the implant surface and the surrounding bone under axial, oblique, and rotational forces. It has been suggested that internal connection implants presented lower stress concentrations than external connection implants in the absence of bone loss around the implants [13]. It has also been highlighted that, since the main factor in stress transmission is considered to be loss of peri-implant bone, the effect of other influencing factors such as implant-abutment connection might be considered ineffective. This may be the reason why the loss of support around the implant compromises the stability of the implant-abutment interface, thus negating the effect of another external variable. In line with this, the present study indicated that higher stress was observed for internal-abutment connection implants compared to external connection in the models with peri-implant bone loss. On the contrary, in models without bone loss, external connection implants showed higher stresses on both the implant surface and cortical bone in the mandible with D2 bone type, but not for the models in the maxilla.

Conclusion

- Higher stress was observed for internal-abutment connection implants compared to external connection in the models with peri-implant bone loss.
- Increased high stress values in the buccal area have marked the critical importance of buccal bone preservation during implant removal procedures.
- Cortical bone can show the maximum stress in the neck region of the implants with peri-implant bone loss compared to cancellous bone under a removal torque value.

Scientific Responsibility Statement

The authors declare that they are responsible for the article's scientific content including study design, data collection, analysis and interpretation, writing, some

of the main line, or all of the preparation and scientific review of the contents and approval of the final version of the article.

Animal and human rights statement
All procedures performed in this study were in accordance with the ethical standards of the institutional and/or national research committee and with the 1964 Helsinki declaration and its later amendments or comparable ethical standards. No animal or human studies were carried out by the authors for this article.

Funding: *None*

Conflict of interest
None of the authors received any type of financial support that could be considered potential conflict of interest regarding the manuscript or its submission.

References
1. Berglundh T, Armitage G, Araujo MG, Avila-Ortiz G, Blanco J, et al. Peri-implant diseases and conditions: Consensus report of workgroup 4 of the 2017 World Workshop on the Classification of Periodontal and Peri-Implant Diseases and Conditions. J Clin Periodontol. 2018;45 (Suppl.20):S286-91. DOI:10.1111/jcpe.12957
2. Anitua E, Piñas L, Begoña L, Alkhraisat MH. Prognosis of Dental Implants Immediately Placed in Sockets Affected by Peri-implantitis: A Retrospective Pilot Study. Int J Periodontics Restorative Dent. 2017;37(5):713-9.
3. Froum S, Yamanaka T, Cho SC, Kelly R, St James S, Elian N. Techniques to remove a failed integrated implant. Compend Contin Educ Dent. 2011;32(7):22-6.
4. Anitua E, Murias-Freijo A, Alkhraisat MH. Conservative implant removal for the analysis of the cause, removal torque, and surface treatment of failed nonmobile dental implants. J Oral Implantol. 2016:42(1);69-77.
5. Geng JP, Tan KB, Liu GR. Application of finite element analysis in implant dentistry: a review of the literature. J Prosthet Dent. 2001;85(6):585-98.
6. Macedo JP, Pereira J, Faria J, Souza JCM, Alves JL, López-López J, et al. Finite element analysis of peri-implant bone volume affected by stresses around Morse taper implants: effects of implant positioning to the bone crest. Comput Methods Biomech Biomed Engin. 2018;21(12):655-62. DOI: 10.1080/10255842.2018.1507025.
7. Misch CE. Bone Classification, Training Keys to Implant Success. Dent Today 1989;8(4):39-44.
8. Schwarz F, Sahm N, Schwarz K, Becker J. Impact of defect configuration on the clinical outcome following surgical regenerative therapy of peri-implantitis. J Clin Periodontol. 2010;37(5):449–55.
9. Albrektsson T. Hard Tissue Implant Interface. Aust Dent J. 2008;53(Suppl.1):S34-8.
10. Vaidya P, Mahale S, Kale S, Patil A. Osseointegration-a Review. J Dental Med Sci. 2017;16(1):45-8.
11. Akca K, Cehreli MC. Biomechanical Consequences of Progressive Marginal Bone Loss around Oral Implants: A Finite Element Stress Analysis. Med Biol Eng Comput. 2006;44(7):527-35.
12. Cinel S, Celik E, Sagirkaya E, Sahin O. Experimental evaluation of stress distribution with narrow diameter implants: A finite element analysis. J Prosthet Dent. 2018;119(3):417-25.
13. Lemos CAA, Verri FR, Noritomi PY, Kemmoku DT, Souza Batista VE, Cruz RS, et al. Effect of bone quality and bone loss level around internal and external connection implants: A finite element analysis study. J Prosthet Dent. 2021;125(1):137.e1-e10.
14. Gupta S, Goyal P, Jain A, Chopra P. Effect of Peri-Implantitis Associated Horizontal Bone Loss on Stress Distribution around Dental Implants–a 3d Finite Element Analysis. Mater Today Proc. 2020;28:1503–9.
15. Dos Santos MBF, Meloto GDO, Bacchi A, Correr-Sobrinho L. Stress distribution in cylindrical and conical implants under rotational micromovement with different boundary conditions and bone properties: 3-D FEA. Comput Methods Biomech Biomed Engin 2017;20(8):893-900.
16. Waechter J, Madruga MDM, Carmo Filho LCD, Leite FRM, Schinestsck AR, Faot F. Comparison between tapered and cylindrical implants in the posterior regions of the mandible: A prospective, randomized, split-mouth clinical trial focusing on implant stability changes during early healing. Clin Implant Dent Relat Res. 2017;19(4):733-41.
17. Baldi D, Lombardi T, Colombo J, Cervino G, Perinetti G, Di Lenarda R, et al. Correlation between Insertion Torque and Implant Stability Quotient in Tapered Implants with Knife-Edge Thread Design. Biomed Res Int. 2018;2018:7201093. DOI: 10.1155/2018/7201093.
18. Udomsawat C, Rungsiyakull P, Rungsiyakull C, Khongkhunthian P. Comparative study of stress characteristics in surrounding bone during insertion of dental implants of three different thread designs: A three-dimensional dynamic finite element study. Clin Exp Dent Res. 2019;5(1):26-37.

How to cite this article:
Ahu Uraz Çörekci, Sila Cagri Isler, Janset Şengül, Berceste Guler, Yücel Özdemir, Deniz Ozbay. *Effect of implant-abutment connections with peri-implant bone defect models under removal torque force: A 3D finite element analysis. nn Clin Anal Med 2023;14(4):358-364*